Real-time navigation for laparoscopic hepatectomy using image fusion of preoperative 3D surgical plan and intraoperative indocyanine green fluorescence imaging

Peng Zhang[1] · Huoling Luo[2] · Wen Zhu[1] · Jian Yang[1] · Ning Zeng[1] · Yingfang Fan[1] · Sai Wen[1] · Nan Xiang[1] · Fucang Jia[2] · Chihua Fang[1]

Abstract

Background Understanding the internal anatomy of the liver remains a major challenge in anatomical liver resection. Although virtual hepatectomy and indocyanine green (ICG) fluorescence imaging techniques have been widely used in hepatobiliary surgery, limitations in their application for real-time navigation persist.

Objective The aim of the present study was to evaluate the feasibility and clinical utility of the novel laparoscopic hepatectomy navigation system (LHNS), which fuses preoperative three-dimensional (3D) models with ICG fluorescence imaging to achieve real-time surgical navigation.

Methods We conducted a retrospective review of clinical outcome for 64 patients who underwent laparoscopic hepatectomy from January 2018 to December 2018, including 30 patients who underwent the procedure using the LHNS (LHNS group) and 34 patients who underwent the procedure without LHNS guidance (Non-LHNS group).

Results There was no significant difference in preoperative characteristics between the two groups. The LHNS group had a significantly less blood loss (285.0 ± 163.0 mL vs. 391.1 ± 242.0 mL; $P = 0.047$), less intraoperative blood transfusion rate (13.3% vs. 38.2%; $P = 0.045$), and shorter postoperative hospital stay (7.8 ± 2.1 days vs. 10.6 ± 3.8 days; $P < 0.001$) than the Non-LHNS group. There was no statistical difference in operative time and the overall complication rate between the two groups. The liver transection line was clearly delineated by the LHNS in 27 patients; however, the projection of boundary was unclear in 2 cases, and in 1 case, the boundary was not clearly displayed by ICG fluorescence imaging.

Conclusions We developed the LHNS to address limitations of current intraoperative imaging systems. The LHNS is hopefully to become a promising real-time navigation system for laparoscopic hepatectomy.

Keywords Laparoscopic hepatectomy · Virtual hepatectomy · Fluorescence · Indocyanine green · Surgical navigation

Peng Zhang, Huoling Luo and Wen Zhu contributed equally to this work.

✉ Nan Xiang
zjyyxn@126.com

✉ Fucang Jia
fc.jia@siat.ac.cn

✉ Chihua Fang
fangch_dr@163.com

1   The First Department of Hepatobiliary Surgery, Guangdong Provincial Clinical and Engineering Center of Digital Medicine, Zhujiang Hospital, Southern Medical University, Guangzhou 510282, China

2   Research Laboratory for Medical Imaging and Digital Surgery, Shenzhen Institutes of Advanced Technology, Chinese Academy of Sciences, Shenzhen 518055, China

Laparoscopic hepatectomy has progressively gained increased acceptance over the past two decades. As a technically demanding approach, it requires that surgeons should not only possess expertise in liver surgery but also comprehend the relationship between hepatic vessels and tumors. The use of laparoscopy has obvious advantages of being a less traumatic procedure with fewer complications and a potentially faster postoperative recovery. Despite these advantages, there are many drawbacks of laparoscopic surgery like lack of tactile perception, restricted vision, and the inability of seeing through the complex internal structure [1, 2]. By three-dimensional (3D) visualization of the liver and virtual hepatectomy, traditional ways of evaluating the positional relationship of blood vessels and measuring the volume of resected liver prior to surgery have been altered.

Nevertheless, several problems have emerged. During the process of applying preoperative 3D surgical planning to the actual operation, issues such as spatial and temporal separation and lack of accuracy still exist [3–5]. Indocyanine green (ICG) fluorescence imaging has obvious advantages in detection of the boundaries of the tumor, identification of small liver tumors, and liver metastases and staining of the drainage area of the portal vein. It has been applied for the real-time navigation of hepatic tumors during liver resection, which cannot be achieved by traditional surgical approach, thereby enhancing the accuracy of surgery. However, ICG fluorescence imaging can be applied only to those lesions located superficially on the liver surface, because the near-infrared light only penetrates tissues to a depth of about 10 mm [6–8]. To perform a safe and effective laparoscopic hepatectomy, it is vital to grasp the positional relationship between the intrahepatic vessels and liver tumors.

To address these issues, we present a multimodal assistant system, the laparoscopic hepatectomy navigation system (LHNS), consisting of a fusion model of computed tomography (CT)-based 3D models with ICG fluorescence images. It is a system for real-time visualization of the relationship between liver lesions and intrahepatic anatomical structures, and the optimal cutting plane that has been preoperatively planned for the actual resection. The range of liver resection can be accurately determined and the preoperative planning based on the simulated resection can be well transformed. The LHNS is a solution that addresses the clinical need of intraoperative real-time navigation for safer and more effective liver resections.

Patients

The subjects comprised a total of 64 patients who had undergone laparoscopic hepatectomy at Zhujiang Hospital, Southern Medical University between January 2018 and December 2018. The inclusion criteria were as follows: (1) age ≥ 18 years, regardless of gender; (2) patients who were diagnosed with liver cancer according to preoperative CT and/or Gd-EOB-DTPA-enhanced magnetic resonance (MR); (3) no vascular invasion, extrahepatic metastasis, or distance metastasis detected according to CT and/or MR; (4) Child–Pugh class A or B liver function; and (5) patients who underwent laparoscopic hepatectomy. The exclusion criteria were as follows: (1) a history of previous abdominal surgery; (2) Child–Pugh class C liver function; and (3) incomplete data. All patients were informed of treatment details including surgical procedures, risks, and complications. Informed consent was obtained from each patient included in the study. The patients were divided into the LHNS group and non-LHNS group. Ultimately, 30 hepatectomy procedures were performed under LHNS guidance and 34 cases

without. The patients with or without LHNS guidance were compared respect to preoperative baseline characteristics, surgical data, postoperative clinical outcomes. Our study protocol was approved by the Institutional Ethics Review Board of Zhujiang Hospital, Southern Medical University (approval code: 2018-GDYK-003). The study was registered at www.clinicaltrials.gov (ClinicalTrials.gov number, NCT03811704).

## Surgical planning based on 3D reconstruction

3D images of the liver, blood vessels, and tumors were created using the Medical Image 3D Visualization System (MI-3DVS, software copyright No: 2008SR18798), based on preoperative CT images. From the 3D reconstructed images, virtual hepatectomy was performed to (1) assess the exact location of the liver tumor and its anatomical relationship to hepatic vasculature; (2) set the surgical margin; (3) determine the corresponding transection plane of hepatic artery, portal vein, and hepatic vein; (4) carry out detailed volumetric analyses; (5) assess the optimal transection plane [3].

Administration of ICG

(1) ICG (0.05–0.10 mg/kg) was injected intravenously 24–72 h prior to surgery. (2) Liver demarcation was identified during operation. Positive staining: ICG was injected intravenously at a dose of 2.5 mg into the tumor-bearing hepatic segment or the portal branches; negative staining: ICG was injected intravenously at a dose of 2.5 mg after clamping the segmental portal pedicle.

Laparoscopic hepatectomy navigation system (LHNS)

The LHNS (software copyright No. 2018SR840555) was developed in collaboration with Shenzhen Institute of Advanced Technology, Chinese Academy of Sciences. It consists of preoperative model segmentation, intraoperative laparoscopic stereo surface reconstruction, intraoperative registration, and intraoperative laparoscopic posture tracking modules (Fig. 1). The LHNS is implemented in C++ and Python using the open-source toolkit on the Windows 10 operating system. These kits include Insight Segmentation and Registration Toolkit (ITK) (www.itk.org), Visualization Toolkit (VTK) [2:www.vtk.org], Open Source Computer Vision Library (OpenCV) [3:www.opencv.org], TensorFlow [4:www.tensorflow.org] and the Medical Imaging Interaction Toolkit (MITK) [9]. We adopted the method
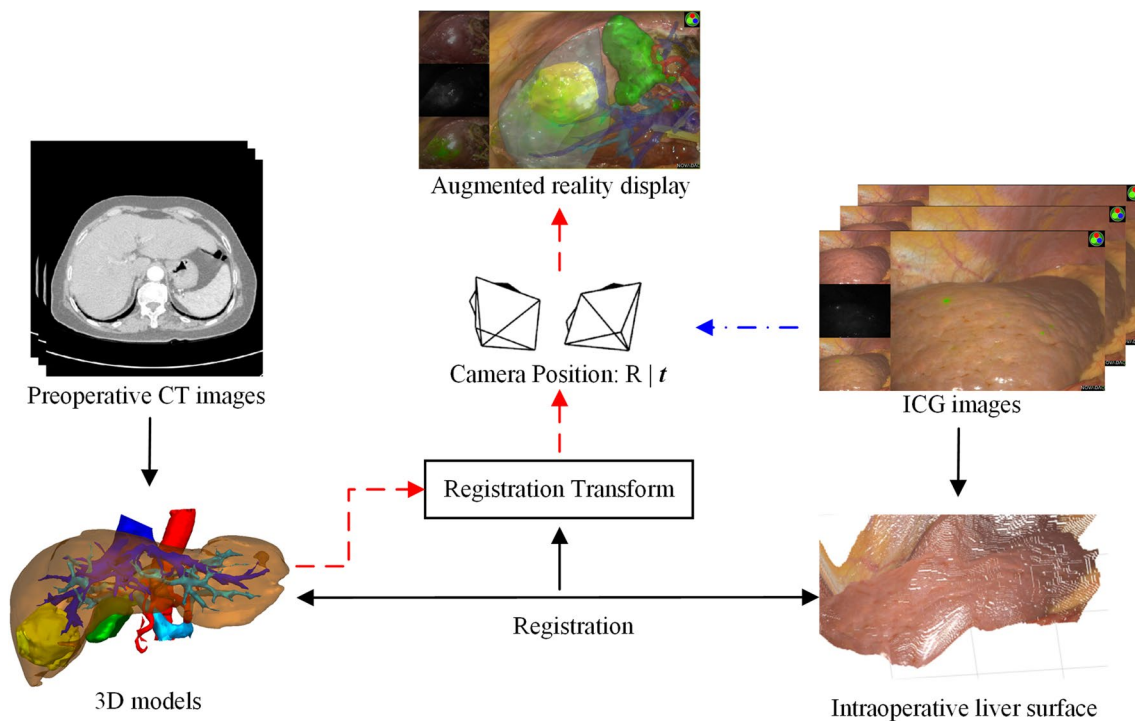
Fig. 1 Framework diagram of the navigation algorithm for the real-time fusion of preoperative 3D models and intraoperative indocyanine green fluorescence image. The display effect of augmented reality for real-time surgical navigation can be obtained through real-time fusion of 3D models reconstructed preoperatively from CT images and intraoperative laparoscopic image or intraoperative indocyanine green fluorescence image

of dense three-dimensional reconstruction of laparoscopic organs base on ORB-SLAM2 [10]. This method can simultaneously estimate the posture of the laparoscopic camera while obtaining 3D information of the organ surface. After the establishment of pneumoperitoneum pressure, the white-light HD mode of Pinpoint endoscopic fluorescence imaging system (Novadaq Technologies Inc., Canada) was used to capture 2–3 s of video images and then the surface model of liver was obtained by 3D dense stereo reconstruction method; then, the model was registered with the preoperative liver surface using Go-ICP method to obtain the spatial transformation matrix between the preoperative CT image space and the intraoperative laparoscopic space [11]. If the automatic registration effect was unsatisfactory, the system would provide a manual registration function. The subsequent fusion would dynamically adjust the preoperative and intraoperative spatial transformation matrix based on the initial registration results, and the posture of the laparoscopic camera estimated by this method. The preoperative model was projected onto the white-light HD image or fluorescent image of laparoscopy under the effect of the transformation matrix, forming the effect of augmented reality display [12].

The signal of laparoscopic image or Pinpoint fluorescence imaging system was first input into a video parser (e-communication system GK310, Guangzhou Guangkang Medical

Technology Co., Ltd., Guangzhou, China), then transmitted to the laptop pre-installed with LHNS system through Epiphan AV.io HD™ video grabber, and then the preoperative reconstructed 3D model was imported into the LHNS. After registration, real-time fusion of 3D model and ICG fluorescence imaging would be displayed simultaneously on the computer monitor (Fig. 2).

Statistical analysis

All statistical analyses were performed using IBM SPSS 22.0 for Windows. Continuous variables were compared using Student's t test, and categorical variables were evaluated using the Chi-square test. The Mann–Whitney U test was used for analyzing the ranked data. $P < 0.05$ was considered as indicative of statistical significance.

Results

The clinicopathological features, surgical parameters and postoperative outcomes of the patients are summarized in Table 1. No significant differences between the two groups are identified. The LHNS group had a less blood loss (285.0 ± 163.0 mL vs. 391.1 ± 242.0 mL; $P = 0.047$), a
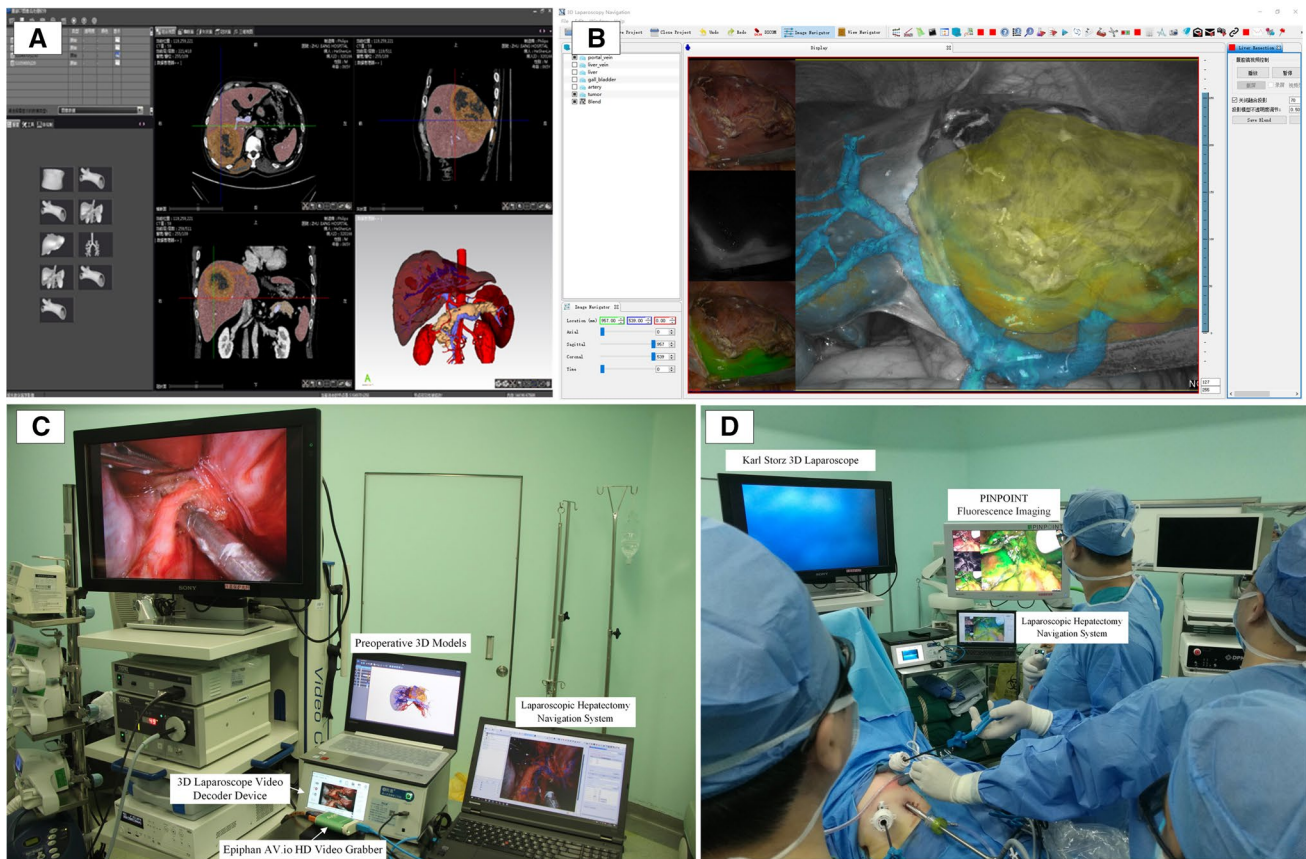
Fig. 2 A Through MI-3DVS, three-dimensional reconstruction of abdominal organs, hepatic artery, hepatic vein, portal vein, and tumor was performed based on CT data; **B** The preoperative reconstructed 3D model was imported into LHNS; **C** Intraoperative scene and use of video decoder device to import laparoscopic images into LHNS; **D** Intraoperative scene and use of video decoder device to import Pinpoint fluorescence imaging into LHNS

less transfusion requirement (13.3% vs. 38.2%; $P = 0.045$), and a shorter postoperative hospital stay (7.8 ± 2.1 days vs. 10.6 ± 3.8 days; $P < 0.001$). There was no significant difference in operative time between these two groups. No accidental bleeding occurred. There were 5 cases of postoperative complications in the LHNS group and 9 cases in the Non-LHNS group. There were no significant differences in the incidence rate of complications between these two groups. All the complications were recovered eventually, and no perioperative death occurred in either group.

The demarcation line or range of resection was clearly projected by the LHNS in 27 patients, undetectable in 2 patients due to large tumor size (> 10 cm) and restricted vision under laparoscopy, and unable to be consecutively identified in 1 patient because of long retention of ICG caused by the cirrhosis and abundant intrahepatic vascular communicating branches. In the LHNS group, the projected 3D images of the tumor and blood vessels showed the important pipeline structures, such as the middle hepatic vein and the variant portal vein branches, which may be encountered during liver resection.

Three exemplar case reports are presented to demonstrate the usefulness of real-time navigation for laparoscopic hepatectomy using image fusion of preoperative 3D surgical plan and intraoperative ICG fluorescence imaging.

Patient 1

A huge tumor was identified in the left lobe of the liver on the preoperative CT (Fig. 3A). Based on the reconstructed preoperative 3D images (Fig. 3B), a left hepatectomy was planned. Intraoperatively, the residual fluorescence in the left lobe was visualized, which resulted from impaired bile excretion in the left hepatic duct that are compressed by the tumor. The demarcation line of the liver surface was identified by direct vision. Real-time fusion of the 3D reconstructed images and the fluorescent images were displayed on a monitor (Fig. 3C). The dissection line was determined based on the preoperative virtual hepatectomy model and the demarcation line by ICG fluorescent signal (Fig. 3D); meanwhile, main branches of the portal vein, hepatic vein, and hepatic artery as well as the location of the tumor were

Table 1 Laparoscopic hepatectomy outcomes between patients with and without using the laparoscopic hepatectomy navigation system (LHNS)

| Variable	LHNS ($n=30$)	Non-LHNS ($n=34$)	P Value
Baseline characteristics			
Age, years, mean $\pm$ SD	55.7 $\pm$ 11.2	52.5 $\pm$ 12.1	0.279
Sex, male/female	23/7	29/5	0.523
HBsAg ($\pm$)	17/13	22/12	0.610
Child–Pugh class (A/B)	27/3	34/0	0.097
Background liver (normal liver/chronic hepatitis/cirrhosis)	14/6/10	12/11/11	0.490
Surgical procedure (n)			0.972
Left hepatectomy	5	4	
Right hepatectomy	4	5	
Central bisectionectomy	2	2	
Right posterior sectionectomy	4	3	
Left extrahepatic lobectomy	1	1	
Partial hepatectomy	14	19	
Operation time, min, mean $\pm$ SD (range)	325.8 $\pm$ 118.1(80–540)	294.7 $\pm$ 100.2(180–540)	0.258
Operative blood loss, ml, mean $\pm$ SD (range)	285.0 $\pm$ 163.0(50–800)	391.1 $\pm$ 242.0(100–1000)	0.047*
Intraoperative blood transfusion, n (%)	4(13.3%)	13(38.2%)	0.045*
Intraoperative adverse events	0	0	
Clearly identify tumor boundary on LSNS images n (%)	27(90.0%)	–	
Postoperative hospital stay, days, mean $\pm$ SD	7.8 $\pm$ 2.1	10.6 $\pm$ 3.8	<0.001*
Pathological findings			0.274
Hepatocellular carcinoma, n	26	33	
Cholangiocarcinoma, n	3	1	
Focal nodular hyperplasia, n	1	0	
Postoperative outcomes (Clavien–Dindo classification)			
Morbidity n (%)	5(16.7%)	9(26.5%)	0.384
Grade I or II n (%)	3(10.0%)	4(11.8%)	
Grade III or IV n (%)	2(6.7%)	5(14.7%)	
Wound infection(n)	0	1	
Lung infection (n)	1	3	
Pleural effusion (n)	2	2	
Seroperitoneum (n)	2	2	
Hemorrhage (n)	0	1	

Some patients have more than one complication

*Significant difference

visualized, which guided the anatomy of the first portal hepatis and the parenchymal dissection. The shape of the residual liver in the actual surgery was basically consistent with that of residual liver in virtual hepatectomy (Fig. 3E). Tumors were not developed in the fluorescence mode. The fluorescence signal on the liver section was ICG excretion disorder (Fig. 3F) caused by tumor compression.
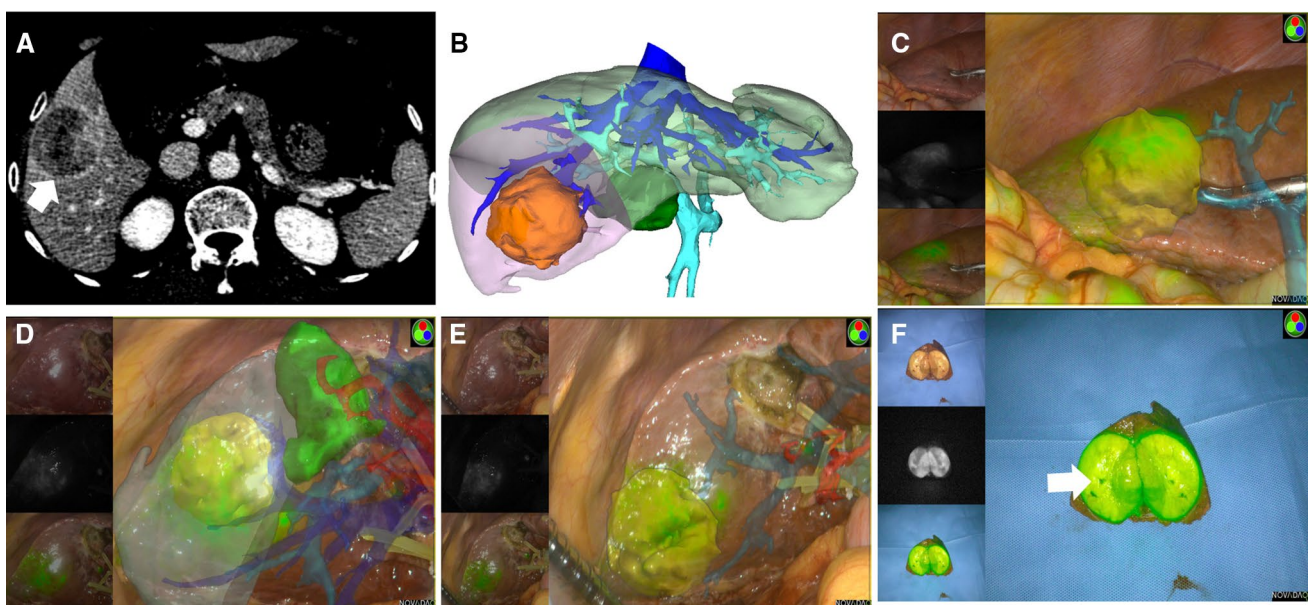
Patient 2

Preoperative CT identified a tumor located in hepatic segments V and VI (Fig. 4A). Based on the reconstructed 3D images, a partial hepatectomy of segments V and VI was planned (Fig. 4B). Intraoperatively, ICG retention was observed around the tumor on the surface of hepatic segments V and VI. The fluorescent images were used as markers to superimpose the preoperative 3D reconstructed model and the ICG fluorescence images in real time (Fig. 4C). The intrahepatic vascular structures were visualized; the distance and relationship of the tumor and important pipelines were evaluated in real time to determine whether a radical excision margin was obtained (Fig. 4D). The branch of the right Glissonian sheath was taped and the blood flow was blocked guided by the 3D reconstructed images (Fig. 4E). The 3D images were adjusted to overlap with the liver in the surgical field, and 2 cm of resection margin was achieved. No residual tumor was detected on the liver section (Fig. 4F). The tumor was partially developed in the fluorescence mode.
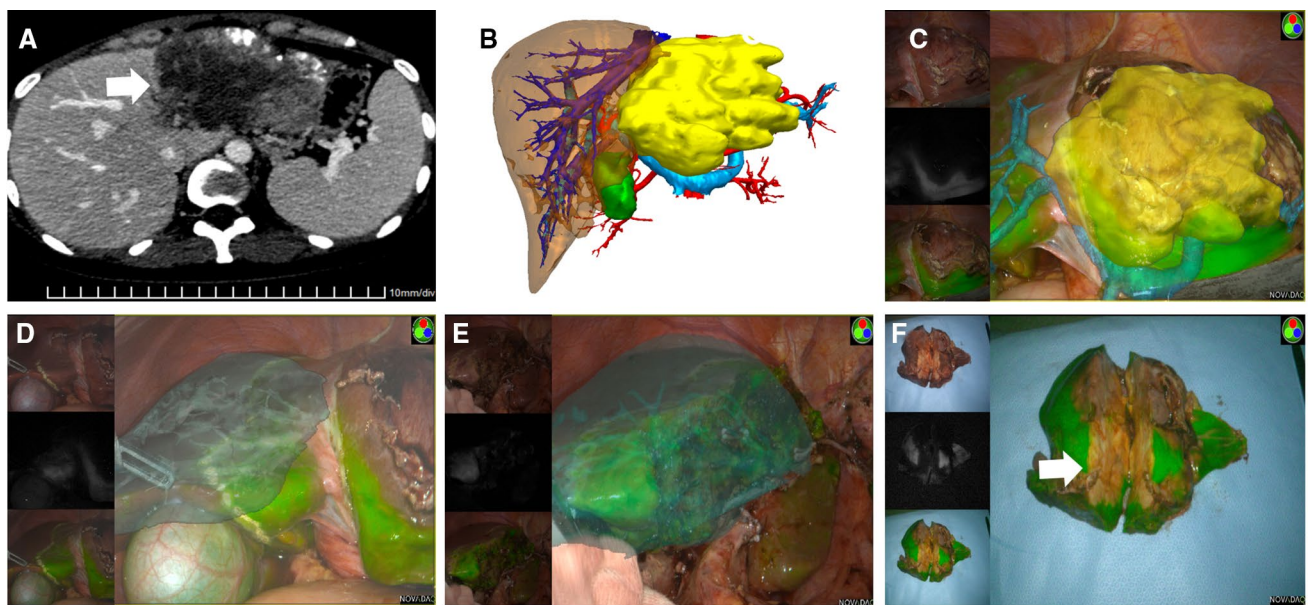
Fig. 3 An anatomic left hemi-hepatectomy for treatment of a hepatocellular carcinoma patient using the Laparoscopic Hepatectomy Navigation System (LHNS) is shown; **A** The preoperative CT showed that the tumor (about 93 mm in diameter) is located in the left lobe of the liver (white bold arrow); **B** A reconstructed 3D model based on preoperative CT image and anatomic left hemi-hepatectomy; **C** Real-time fusion of 3D image, Indocyanine Green fluorescence and laparoscopic images of tumors and portal vein; **D** Determination of resection line of liver by ICG fluorescence image; **E** 3D projection of patients' residual liver; **F** No fluorescence development was found in the dissected specimen

Fig. 4 A Partial hepatectomy for treatment of a hepatocellular carcinoma patient using the Laparoscopic Hepatectomy Navigation System (LHNS) is shown; **A** The preoperative CT shows that the tumor (about 43 mm in diameter) is located in the right lobe of the liver (white bold arrow); **B** A reconstructed 3D model based on preoperative CT images is 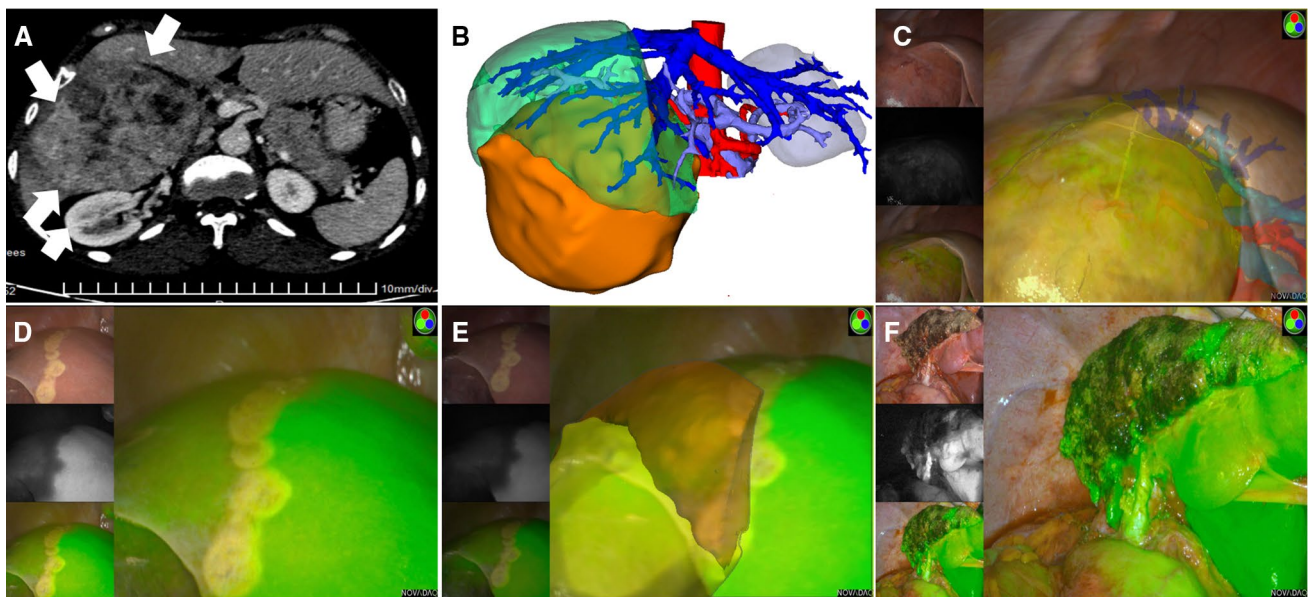shown, and partial hepatectomy is planned; **C** 3D model of tumor and portal vein was projected onto the ICG fluorescence image on the surface of liver; **D** The 3D images of tumor, hepatic artery, and portal vein were projected onto the surface of the liver; **E** The 3D model of preoperative virtual hepatectomy was projected onto the surface of the liver; **F** Part of tumor developed under fluorescence in the dissected specimen

Patient 3

Preoperative CT localized a huge tumor in the right lobe of the liver (Fig. 5A). Based on the reconstructed preoperative 3D images (Fig. 5B), a right hepatectomy was planned. Intraoperatively, the residual fluorescence around the tumor was observed, which resulted from ICG excretion disorders in the surrounding normal tissues that were compressed by the tumor. (Figure 5C). The 3D reconstructed model of the portal hepatis was superimposed with the laparoscopic image in real time. The branch of the right Glissonian sheath was taped and blood flow was blocked. The right hepatic artery and the right portal vein were ligated and blocked (Fig. 5D). ICG was injected intravenously. Fluorescent images obtained were projected onto the liver surface using the LHNS. Based on real-time fusion of preoperative 3D imaging and ICG fluorescent images, the dissection line was determined (Fig. 5E). Main branches of the hepatic portal vein, hepatic artery, and hepatic artery as well as the location of the tumor were visualized through the 3D reconstructed model. During parenchymal dissection, the transection plane was monitored and timely corrected by the fusion images of the 3D model and ICG fluorescence image (Fig. 5F).

Discussion

Because of technical innovations and experience accumulation in liver surgery, the indications for laparoscopic hepatectomy are almost the same as the open hepatectomy. The advantages of the laparoscopic surgery over the laparotomy include a reduced pain, a shorter operative time and hospital stay, less complications, and a faster recovery. However, laparoscopic liver surgery is still limited by lack of hand tactile feedback, narrowed operating space, and limited visual field and visual angle of an endoscope [13–15]. These issues have been addressed to some extent by some of the most promising technologies developed in recent years, including CT, MR imaging, intraoperative ultrasound, ICG fluorescence imaging [16], augmented reality [17], and mixed reality [18]. In this study, we present a novel laparoscopic hepatectomy navigation system (LHNS), with which real-time navigation for laparoscopic hepatectomy can be achieved through the fusion of preoperative 3D model and intraoperative ICG fluorescence image. The liver resection guided by the LHNS is more accurate and reliable compared to the conventional image-guided surgery. The LHNS is superior because surgeons can concentrate on the surgical field without having to shift their vision to the laparoscopic image, ICG image and preoperative 3D image during the operation, which has eliminated the factors that lead to the operator's hand–eye

Fig. 5 An anatomic right hemi-hepatectomy for treatment of a hepatocellular carcinoma patient using the Laparoscopic Hepatectomy Navigation System(LHNS) is shown; **A** Preoperative CT showed that tumor (about 104 mm) is located in the right lobe of liver (white bold arrow); **B** Reconstructed 3D model based on preoperative CT images, and right hemi-hepatectomy; **C** 3D images of tumor, portal vein, and hepatic artery were projected onto the ICG fluorescence image on the surface of liver; **D** Determination of the resection line of liver by ICG fluorescence image; **E** 3D model of preoperative virtual hepatectomy and tumor were projected onto the surface of liver; **F** No residual tumor and bile leakage on liver cross section were detected by fluorescence

incoordination due to the spatial and temporal separation of 3D image-guided surgery. This procedure helps to realize real-time navigation of multimodal images during laparoscopic hepatectomy.

3D visualization of organs enhances the understanding of complex anatomical structures; virtual liver resection based on the reconstructed 3D models has been widely used these years. However, because of the non-rigid registration approach for hepatobiliary surgery, respiratory motion and deformation of the liver during the surgical procedures leads to inaccuracies of subsequent image-guided surgical navigation [3, 5, 19, 20]. Preoperatively, 3D images of the intrahepatic structure and tumor were generated using a 3D image processing software; intraoperatively, through a fast registration procedure, the 3D images were integrated with the current patient and surgical instrument position into one coordinate system. To track the position of surgical instruments, the optical tracking system (Polaris Spectra optical tracker, Northern Digital Inc., Waterloo, Ontario, Canada) was used. According to the relative positional relationship between surgical instruments and lesions in the 3D model, surgeons can understand the important anatomical structure near the operating site in real time, which enhances the accuracy and safety of liver surgery [21]. Despite these virtues, there are certain drawbacks in the tracking system, such as light occlusion and long configuration time, which easily affect the surgical process. While in the LHNS, ORB-SLAM2 was used to acquire the real-time camera pose. After the first registration, the subsequent model position was adjusted according to the camera's pose in real time. Since we do not use an external tracking system during navigation, the registration time required is greatly reduced. The setup time of the current navigation system is mainly derived from the reconstruction of the intraoperative liver surface and the registration with the preoperative liver model. The system setup before navigation only takes about 30 s. The setting up and use of the navigation is trained by the engineer before the operation, and can be performed independently by surgeons during the operation. Currently, the navigation of abdominal surgery is mostly realized by augmented reality technology and mixed reality technology. The preoperative 3D images of the liver are projected onto the patient's body and superimposed with the patient's real liver during the liver surgery, which helps the surgeons to observe the overlapped images of 3D models and actual surgical sites. It enables surgeons to visualize the complex liver anatomy, allowing them to predict and judge the important blood vessels or anatomical structures to be encountered in advance, thereby greatly improving the safety of operation [18, 22].

ICG is a near-infrared fluorescent dye certified by FDA in the USA, which is mainly metabolized by hepatocytes and excreted through biliary tract [23]. The pathological changes at cellular and molecular levels in living organisms are reflected using ICG fluorescence imaging. The definition of the tumor boundary at the cellular level can be preliminarily achieved. During operation, dynamic observation can be carried out, and the transection plane can be adjusted and corrected according to the fluorescence boundary of hepatic parenchyma [16]. At present, ICG fluorescence imaging has obvious advantages in the recognition of the biliary system, the definition of liver tumor boundary, the detection of small lesions, the intraoperative real-time navigation, and portal vein drainage area identification [7]. The fluorescence imaging system originally developed for clinical use consists of a small control unit and a charge coupled device camera that filters out light at wavelengths below 820 nm and 36 diodes capable of emitting wavelength 760 nm. Fluorescent image data are transmitted to a personal computer through video capture card to display and store [6]. Later, the technology has been developed to fuse images of macroscopic surgical fields and near-infrared images into a single display. However, during laparotomy, surgeons are required to shift between the direct vision and the fusion images. Therefore, the fusion ICG fluorescence imaging system may be more suitable for laparoscopic surgery [16]. Recently, a new Medical Imaging Projection System (MIPS) integrates the ICG fluorescence imaging and active projection mapping for liver resection. Continuous 3D projection combined with fluorescence imaging can effectively determine the line of resection, identify anatomical markers of hepatic parenchyma and guide the incision of deep hepatic parenchyma [24]. Our LHNS integrates preoperative models and ICG images on the same computer monitor and expands the application of ICG fluorescence imaging technology. It has the following advantages over traditional intraoperative image-guided techniques: surgeons can focus on the same monitor without distraction because of changing the field of vision in the different monitors; the plane of preoperative virtual hepatectomy is implemented into actual operation, which is a good transformation of preoperative surgical planning; the positional relationship between tumor and intrahepatic duct is well understood in real time according to the 3D model of the overlapping image, which can guide the excision of liver parenchyma and reduce the injury of important ducts; ICG fluorescence signal on the liver surface can be used as a marker for the registration of the 3D model with the liver, which can solve the problems of complicated instrument connection, limited space and long installation of the system.

In our study, the two groups showed no apparent difference in patient demographics, operation time, and postoperative complications. However, there were some differences between the two groups in operative blood loss, intraoperative blood transfusion, and postoperative hospital stays. Although there was no significant difference in complications between the two groups, the overall complication rate in the LHNS group tended to be lower than that in the

Non-LHNS group (16.7 vs. 26.5%, $P = 0.384$). Compared with the LHNS group, the Non-LHNS group had a higher incidence of incision infection and pulmonary infection; meanwhile, current studies revealed that postoperative infective complications decreased long-term overall survival and recurrence-free survival in patients treated with liver resection for hepatocellular carcinoma [25]. In addition, previous studies have demonstrated that perioperative blood transfusion is one of the adverse factors that affect the perioperative recovery and long-term survival of the patient [26–28]. Therefore, we believe that the low incidence of complications in the LHNS group is mainly related to the reduction of intraoperative bleeding and blood transfusion, which may help to improve the long-term overall survival and recurrence-free survival of patients undergoing liver resection for malignant tumors. In the LHNS group, augmented reality technology was used to superimpose the 3D images onto the surgical field. These superimposed virtual images guided the anatomy of the porta hepatis and parenchymal transection. The branches of the main hepatic and portal veins to be encountered on the transection plane can be strategically identified with greater accuracy, preventing major intraoperative bleeding caused by vascular injury. Hemorrhage has always been a major problem encountered during laparoscopic hepatectomy [29], and it is the main cause of conversion to open surgery. The patients with conversion of laparoscopic surgery to open surgery showed a worse postoperative outcome, higher complications, and higher perioperative mortality than those with complete laparoscopic surgery [30, 31]. Positional registration of the 3D model, the fluorescent image and the real-time anatomical site was attained by the LHNS. The location and scope of the lesion were displayed intuitively by the fluorescent signal. The adjacent relationship between the lesion and its important adjacent organs were identified by the projection of the 3D model. The LHNS allows surgeons to determine the variant blood vessels, the branches of the hepatic vein and portal vein during laparoscopic hepatectomy, which, therefore, could prevent and reduce intraoperative bleeding.

In patient 1, ICG was distributed in the excised liver area, and the tumor protruded through the surface of the liver. The 3D model of the tumor and the portal vein (Fig. 3C), and the demarcation line based on preoperative virtual hepatectomy were projected onto the liver surface. In comparison, the fluorescent signal that formed by ICG retention in the liver showed that the demarcation between the left and right lobe of the liver was not a straight line (Fig. 3D). In patient 2, ICG aggregated in the target area for resection, which was considered ICG excretion disorder due to compression of the surrounding liver tissue by the tumor. The fluorescent signal provided markers for projection of the tumor (Fig. 4C). From the projected 3D image, the intrahepatic location of the tumor and the portal vein were identified

(Fig. 4D); meanwhile, the range of the resection area by virtual liver resection was projected onto the actual operation (Fig. 4E). In patient 3, ICG was partially accumulated in the tumor, but the tumor did not compress the hepatic duct to cause wide distribution of ICG in the target area for resection. For example, in patient 1, the 3D model was projected onto the liver surface to show the relationship between the tumor and intrahepatic vessels (Fig. 5C), and the resection line could be determined by ICG images and the ischemic line (Fig. 5D). The 3D model of the tumor and preoperative virtual hepatectomy could not be completely superimposed in the actual operation due to pneumoperitoneum pressure and liver deformation (Fig. 5E). However, ICG images can guide the parenchymal dissection in real time. No residual tumor and bile leakage on liver cross section were detected by fluorescence (Fig. 5F).

The demarcation line could not be detected using the LHNS in 3 cases. In 2 cases, the tumor was huge (103 mm in diameter) and located in the right lobe of liver. The right and left lobes of the liver where the tumor was located could not be displayed simultaneously due to the restricted space and field of view and the effect of pneumoperitoneum under laparoscope leading to inaccurate identification of the demarcation line by projection, while the demarcation line could be clearly displayed through peripheral vein injection of ICG after blocking the right branch of portal vein. In order to improve the detection and application effect of ICG in large tumors leading to portal vein obstruction, ICG can be injected before operation. During operation, tumor location can be identified by fluorescent signals. When large tumors compress normal liver tissues, the delayed excretion of ICG presents circular fluorescent signals surrounding the tumors [32, 33]. When tumor compression causes the obstruction of the portal vein, anatomical hepatectomy with ICG positive staining may be difficult. Negative staining can be used to preserve the lateral hepatic segment. In the other case, ICG injected preoperatively was still diffused on the liver surface in patients with cirrhosis who underwent right hepatectomy. The demarcation line could be temporarily displayed on the liver surface through peripheral vein injection of ICG after blocking the right branch of portal vein; then, ICG was circulated to the whole liver through the communicating branch of portal vein. Therefore, ICG staining may not be able to clearly identify the demarcation line during hepatectomy, while the projection of preoperative 3D model provides an effective solution to this problem. Direct projection of the 3D model the liver surface through the LHNS can guide the anatomy and transection of Glissonian sheath in the first porta hepatis. At the same time, according to the range of ICG staining, the transection plane can be adjusted in real time according to the liver parenchymal staining. The demarcation line of the liver parenchyma in some patients becomes less clear with the prolongation of staining time.

The image projection provides real-time and continuous monitoring and timely correction of the transection plane to ensure safe surgical margins, which, therefore, could maximize the functional liver volume and achieve the anatomical, functional, and radical hepatectomy. In addition, our current experience suggests that the application of the LHNS has profound clinical significance—especially for tumors with complex intrahepatic positional relationship—such as the presence of hepatic artery, portal vein, and hepatic vein variation in the liver, the proximity of tumors to important vascular systems, the severe distortion of intrahepatic vessels caused by tumor compression, and the presence of small tumors located in the deep liver parenchyma which are difficult to be detected during operation. Intraoperative image fusion techniques could reduce bleeding and enhance the safety of surgery through avoiding the injury of important pipeline structure.

Limitations

The main limitation of this study is its retrospective nature, with the inherent risk of strong selection bias. Besides, the small sample size for the study group and short follow-up time are believed to have an impact on the study to some extent. Therefore, further research is required to include more research objects and observation indexes, and further long-term research will be valuable to clarify the long-term outcome of the malignant tumors to know the advantages in survival. With the advent of digital and intelligent liver surgery [34], it is hoped that in the near future, the advantages of the LHNS in laparoscopic hepatectomy will become more obvious with the extension of clinical application.

Conclusions

To sum up, the fusion of 3D model with ICG florescence imaging through the LHNS can provide convenient and reliable intraoperative multimodal image guidance for laparoscopic hepatectomy, which compensates for the defects of tactile sense and visual fields to some extent, thereby enhancing the safety of operation. Our next step is to address the reduced accuracy of real-time navigation caused by liver deformation due to factors such as pneumoperitoneum pressure, respiration, heartbeat, and surgical procedures. There is also a need for a prospective or randomized large-scale clinical study to confirm that LHNS-guided laparoscopic hepatectomy can enhance the accuracy of surgery and reduce postoperative complications compared with traditional laparoscopic hepatectomy.

Compliance with ethical standards

References

1. Buell JF, Cherqui D, Geller DA, O'Rourke N, Iannitti D, Dagher I, Koffron AJ, Thomas M, Gayet B, Han HS, Wakabayashi G, Belli G, Kaneko H, Ker CG, Scatton O, Laurent A, Abdalla EK, Chaudhury P, Dutson E, Gamblin C, D'Angelica M, Nagorney D, Testa G, Labow D, Manas D, Poon RT, Nelson H, Martin R, Clary B, Pinson WC, Martinie J, Vauthey JN, Goldstein R, Roayaie S, Barlet D, Espat J, Abecassis M, Rees M, Fong Y, McMasters KM, Broelsch C, Busuttil R, Belghiti J, Strasberg S, Chari RS (2009) The international position on laparoscopic liver surgery: The Louisville Statement, 2008. Ann Surg 250(5):825–830
2. Kawaguchi Y, Fuks D, Kokudo N, Gayet B (2018) Difficulty of laparoscopic liver resection. Ann Surg 267(1):13–17
3. Fang C, Tao H, Yang J, Fang Z, Cai W, Liu J, Fan Y (2015) Impact of three-dimensional reconstruction technique in the operation planning of centrally located hepatocellular carcinoma. J Am Coll Surg 220(1):28–37
4. Nakayama K, Oshiro Y, Miyamoto R, Kohno K, Fukunaga K, Ohkohchi N (2017) The effect of three-dimensional preoperative simulation on liver surgery. World J Surg 41(7):1840–1847
5. Mise Y, Hasegawa K, Satou S, Shindoh J, Miki K, Akamatsu N, Arita J, Kaneko J, Sakamoto Y, Kokudo N (2018) How has virtual hepatectomy changed the practice of liver surgery?: experience of 1194 virtual hepatectomy before liver resection and living donor liver transplantation. Ann Surg 268(1):127–133
6. Ishizawa T, Fukushima N, Shibahara J, Masuda K, Tamura S, Aoki T, Hasegawa K, Beck Y, Fukayama M, Kokudo N (2009) Real-time identification of liver cancers by using indocyanine green fluorescent imaging. Cancer 115(11):2491–2504
7. Baiocchi GL, Diana M, Boni L (2018) Indocyanine green-based fluorescence imaging in visceral and hepatobiliary and pancreatic surgery: State of the art and future directions. World J Gastroenterol 24(27):2921–2930
8. Koch M, Ntziachristos V (2016) Advancing surgical vision with fluorescence imaging. Annu Rev Med 67:153–164
9. Nolden M, Zelzer S, Seitel A, Wald D, Muller M, Franz AM, Maleike D, Fangerau M, Baumhauer M, Maier-Hein L, Maier-Hein KH, Meinzer HP, Wolf I (2013) The medical

imaging interaction toolkit: challenges and advances: 10 years of open-source development. Int J Comput Assist Radiol Surg 8(4):607–620

10. Mahmoud N, Collins T, Hostettler A, Soler L, Doignon C, Montiel J (2018) Live tracking and dense reconstruction for hand-held monocular endoscopy. IEEE Trans Med Imag 38(1):79–89

11. Yang J, Li H, Campbell D, Jia Y (2016) Go-ICP: a globally optimal solution to 3D ICP point-set registration. IEEE Trans Pattern Anal Mach Intell 38(11):2241–2254

12. Mahmoud N, Collins T, Hostettler A, Soler L, Doignon C, Montiel J (2019) Live tracking and dense reconstruction for handheld monocular endoscopy. IEEE Trans Med Imag 38(1):79–89

13. Cherqui D (2015) Laparoscopic liver resection: a new paradigm in the management of hepatocellular carcinoma? J Hepatol 63(3):540–542

14. Yoon YI, Kim KH, Kang SH, Kim WJ, Shin MH, Lee SK, Jung DH, Park GC, Ahn CS, Moon DB, Ha TY, Song GW, Hwang S, Lee SG (2017) Pure laparoscopic versus open right hepatectomy for hepatocellular carcinoma in patients with cirrhosis: a propensity score matched analysis. Ann Surg 265(5):856–863

15. Moris D, Vernadakis S (2018) Laparoscopic hepatectomy for hepatocellular carcinoma: the opportunities, the challenges, and the limitations. Ann Surg 268(1):e16

16. Inoue Y, Arita J, Sakamoto T, Ono Y, Takahashi M, Takahashi Y, Kokudo N, Saiura A (2015) Anatomical liver resections guided by 3-dimensional parenchymal staining using fusion indocyanine green fluorescence imaging. Ann Surg 262(1):105–111

17. Conrad C, Fusaglia M, Peterhans M, Lu H, Weber S, Gayet B (2016) Augmented reality navigation surgery facilitates laparoscopic rescue of failed portal vein embolization. J Am Coll Surg 223(4):e31–e34

18. Sauer IM, Queisner M, Tang P, Moosburner S, Hoepfner O, Horner R, Lohmann R, Pratschke J (2017) Mixed reality in visceral surgery: development of a suitable workflow and evaluation of intraoperative use-cases. Ann Surg 266(5):706–712

19. Marescaux J, Clement JM, Tassetti V, Koehl C, Cotin S, Russier Y, Mutter D, Delingette H, Ayache N (1998) Virtual reality applied to hepatic surgery simulation: the next revolution. Ann Surg 228(5):627–634

20. Fang C, Liu J, Fan Y, Yang J, Xiang N, Zeng N (2013) Outcomes of hepatectomy for hepatolithiasis based on 3-dimensional reconstruction technique. J Am Coll Surg 217(2):280–288

21. Peterhans M, Vom BA, Dagon B, Inderbitzin D, Baur C, Candinas D, Weber S (2011) A navigation system for open liver surgery: design, workflow and first clinical applications. Int J Med Robot 7(1):7–16

22. Tang R, Ma LF, Rong ZX, Li MD, Zeng JP, Wang XD, Liao HE, Dong JH (2018) Augmented reality technology for preoperative planning and intraoperative navigation during hepatobiliary surgery: a review of current methods. Hepatobiliary Pancreat Dis Int 17(2):101–112

23. Ishizawa T, Masuda K, Urano Y, Kawaguchi Y, Satou S, Kaneko J, Hasegawa K, Shibahara J, Fukayama M, Tsuji S, Midorikawa Y, Aburatani H, Kokudo N (2014) Mechanistic background and clinical applications of indocyanine green fluorescence imaging of hepatocellular carcinoma. Ann Surg Oncol 21(2):440–448

24. Nishino H, Hatano E, Seo S, Nitta T, Saito T, Nakamura M, Hattori K, Takatani M, Fuji H, Taura K, Uemoto S (2018) Real-time navigation for liver surgery using projection mapping with indocyanine green fluorescence: development of the novel medical imaging projection system. Ann Surg 267(6):1134–1140

25. Yang T, Liu K, Liu CF, Zhong Q, Zhang J, Yu JJ, Liang L, Li C, Wang MD, Li ZL, Wu H, Xing H, Han J, Lau WY, Zeng YY, Zhou YH, Gu WM, Wang H, Chen TH, Zhang YM, Zhang WG, Pawlik TM, Wu MC, Shen F (2019) Impact of postoperative infective complications on long-term survival after liver resection for hepatocellular carcinoma. Br J Surg 106(9):1228–1236

26. Yamamoto J, Kosuge T, Takayama T, Shimada K, Yamasaki S, Ozaki H, Yamaguchi N, Mizuno S, Makuuchi M (1994) Perioperative blood transfusion promotes recurrence of hepatocellular carcinoma after hepatectomy. Surgery 115(3):303–309

27. Katz SC, Shia J, Liau KH, Gonen M, Ruo L, Jarnagin WR, Fong Y, D'Angelica MI, Blumgart LH, DeMatteo RP (2009) Operative blood loss independently predicts recurrence and survival after resection of hepatocellular carcinoma. Ann Surg 249(4):617–623

28. Harada N, Shirabe K, Maeda T, Kayashima H, Ishida T, Maehara Y (2015) Blood transfusion is associated with recurrence of hepatocellular carcinoma after hepatectomy in child–pugh class a patients. World J Surg 39(4):1044–1051

29. Kawaguchi Y, Nomi T, Fuks D, Mal F, Kokudo N, Gayet B (2016) Hemorrhage control for laparoscopic hepatectomy: technical details and predictive factors for intraoperative blood loss. Surg Endosc 30(6):2543–2551

30. Goh BKP, Chan C, Wong J, Lee S, Lee VTW, Cheow P, Chow PKH, Ooi LLPJ, Chung AYF (2015) Factors associated with and outcomes of open conversion after laparoscopic minor hepatectomy: initial experience at a single institution. Surg Endosc 29(9):2636–2642

31. Halls MC, Cipriani F, Berardi G, Barkhatov L, Lainas P, Alzoubi M, D'Hondt M, Rotellar F, Dagher I, Aldrighetti L, Troisi RI, Edwin B, Abu Hilal M (2018) Conversion for unfavorable intraoperative events results in significantly worse outcomes during laparoscopic liver resection. Ann Surg 268(6):1051–1057

32. Lim C, Vibert E, Azoulay D, Salloum C, Ishizawa T, Yoshioka R, Mise Y, Sakamoto Y, Aoki T, Sugawara Y (2014) Indocyanine green fluorescence imaging in the surgical management of liver cancers: current facts and future implications. J Visc Surg 151(2):117–124

33. Alfano MS, Molfino S, Benedicenti S, Molteni B, Porsio P, Arici E, Gheza F, Botticini M, Portolani N, Baiocchi GL (2019) Intraoperative ICG-based imaging of liver neoplasms: a simple yet powerful tool preliminary results. Surg Endosc 33(1):126–134

34. Fang C, Zhang P, Qi X (2019) Digital and intelligent liver surgery in the new era: prospects and dilemmas. EbioMedicine 41:693–701